Physica A 487 (2017) 111–124

Contents lists available at ScienceDirect

Physica A

journal homepage: www.elsevier.com/locate/physa

# Collective dynamics in heterogeneous networks of neuronal cellular automata

Kaustubh Manchanda [a,*], Amitabha Bose [b], Ramakrishna Ramaswamy [c]

[a] Department of Mathematics, Indian Institute of Science, Bangalore 560 012, India
[b] Department of Mathematical Sciences, New Jersey Institute of Technology, Newark, NJ 01702, United States
[c] School of Physical Sciences, Jawaharlal Nehru University, New Delhi 110 067, India

## HIGHLIGHTS

- Heterogeneity on random sites alters network dynamics qualitatively and quantitatively.
- Higher degree nodes with heterogeneities have more chances of sustaining periodicity.
- Network activity curves agree with simulations from a semi-annealed approximation.

## ARTICLE INFO

*Article history:*
Received 30 November 2016
Received in revised form 7 June 2017
Available online 3 July 2017

*Keywords:*
Discrete dynamics
Periodic activity
Binary mixtures
Network motif
Boolean Lyapunov exponent
Semi-annealed approximation

## ABSTRACT

We examine the collective dynamics of heterogeneous random networks of model neuronal cellular automata. Each automaton has $b$ active states, a single silent state and $r-b-1$ refractory states, and can show 'spiking' or 'bursting' behavior, depending on the values of $b$. We show that phase transitions that occur in the dynamical activity can be related to phase transitions in the structure of Erdős–Rényi graphs as a function of edge probability. Different forms of heterogeneity allow distinct structural phase transitions to become relevant. We also show that the dynamics on the network can be described by a semi-annealed process and, as a result, can be related to the Boolean Lyapunov exponent.



## 1. Introduction

As has increasingly been recognized in the past decades, the network paradigm is a useful one within which to understand and study a very large variety of natural systems [1–6]. These ideas have been applied in diverse contexts, with nodes representing entities ranging from neurons [7], genes [8,9], and humans [10], to animals [11], power grids [12], railway stations [13] etc. Depending upon how these nodes interact with each other, the connecting links can be unidirectional or bidirectional, and further, can have interesting topological structure. It has thus been found necessary and useful to study different *types* of networks, ranging from purely random networks such as that described by Erdős and Rényi (ER) [14], to highly structured networks with a power-law degree distribution [15], ordered networks in which some links are disordered [16], modular networks, and so on. Each class of network has distinct geometric properties such as the degree distribution or the clustering coefficient [16].

In this paper, we study the collective dynamics of model neuronal systems on an ER network on which nodes are coupled bidirectionally with probability $p$. A simplified description of a neuron is afforded by the so called $(r : b)$ automaton that has

* Corresponding author.
*E-mail address:* kaustubh011184@gmail.com (K. Manchanda).

http://dx.doi.org/10.1016/j.physa.2017.06.021
0378-4371/

$b$ active states, a single silent state, and $r - b - 1$ refractory states [17], and we study networks with such an automaton at each node. When $b = 1$, the node has one active state and mimics a spiking neuron, while when $b > 1$, the node has several active states and behaves like a bursting neuron. At any time step a node can be in the refractory, silent or active state. As will be described in detail below, the state of the node is updated in discrete time depending on two factors: its current state and the state of the nodes to which it is coupled. We are interested in computing the probability that an initial condition lies on a trajectory that converges to a period orbit of the dynamics, which we denote by $A_f$.

In an earlier work involving ER networks with homogeneous nodes [17], we have studied the dependence of the dynamics on three different aspects of the network: the topology that can be tuned by the probability $p$, the rules for interaction between the nodes, and the value of $b$, namely whether the node corresponded to a spiking or bursting neuron [17,18]. Of the many possible nodal interaction rules, we considered two extremes, namely simple loading (SL) and majority rule (MR), wherein a single (at least half of the) active neighbor(s) of a silent node causes it to become active at the next time step.

In this paper, we focus our attention on how the dynamics depends on the level of heterogeneity in the graph. Since there are a variety of ways in which heterogeneity can be introduced, we restrict our attention to the following cases,

1. Heterogeneity in intrinsic nodal properties: In a neuronal network all neurons need not be identical. Different neurons can spend differing amounts of time in active or refractory states. This motivates the study of a network with heterogeneous nodal dynamics [19], and here, starting with a network with all nodes having $(r : b)$ automata, we replace a random fraction of nodes with $(r' : b')$ automata. Results for the case when all automata on the random networks are identical are already known [17].
2. Heterogeneity in nodal interaction rules distributed randomly: We include the possibility of excitation at a fraction $x$ of the nodes, chosen randomly, occurring via the SL rule, and at $(1 - x)$ through the MR interaction rule. In earlier work [17], all nodes had the same rule, *i.e.* $x = 0$ or 1.
3. Heterogeneity distributed at high degree nodes: We consider finite size networks such that the degree distribution at nodes is not necessarily uniform and examine the difference in the dynamics when the two forms of heterogeneity are at low or high degree nodes.

To analyze these cases, we shall first discuss and prove some results on small networks of either two or three nodes. Using these results and our prior work [17], we can predict in many cases how heterogeneity affects the dynamics of a larger network. We use simulations to validate those predictions. Additionally, the process of calculating $A_f$ is quite similar to a semi-annealed process [20,21], which itself is related to calculating stability boundaries in quenched and annealed networks [22,23]. In specific cases, the large $N$ behavior of the annealed and semi-annealed network approximates the behavior of the quenched system. The stability of these networks is determined by calculating a Boolean Lyapunov exponent (BLE) [24]. In Section 4, we make use of a calculation similar to the semi-annealed approximation and show in simulations that this approximation, $A_f$ and the BLE yield qualitatively similar results. The automaton model and the ER network are discussed in Section 2. Analytical results on small homogeneous network motifs are presented in Section 3. Results are shown for small and large heterogeneous mixtures of $(r : b)$ and $(r' : b')$ automata in Section 4, and the study is summarized in Section 5.

## 2. Neuronal automata on networks

A random graph can be constructed by fixing the number of nodes, $N$, each pair of which is connected with probability $p$. As is well known [14], the degree distribution is binomial with the average degree of each node being equal to $Np$ for large $N$.

Each node of the network is occupied by an automaton that mimics neuronal activity in the following sense. The automaton has $r$ states of which $b$ are denoted "active", $m = r - b - 1$ are "refractory" and there is a single silent state. As described earlier [17,18], it is convenient to represent the silent state by 0, the refractory states as the negative integers $-m, \ldots -1$, and the active states as positive integers, $1 \ldots b$. At any time-step $t$, therefore, the state of an automaton at node $i$, denoted by $\sigma_i(t)$ can take an integer value $\in [-m, b]$.

It is useful to differentiate $(r : b)$ automata by the relative times spent in the active state during a complete cycle. When $r > 2b$, nodes spend a longer time in the refractory phase, while if $r \leq 2b$, the active phase is longer. We examine two specific cases: a spiking neuron with $b = 1$, and a "bursting" neuron with $r \leq 2b$ and $b > 1$. For bursting nodes, we shall mostly focus on the case when the neuron has only one refractory state so that $r = b + 2$. We define $f = b/r$ as the fraction of states that are active.

The nodal dynamics obey the following local rules.

1. If the node is at the end of its active period it transits to the start of the refractory state, namely if $\sigma_i(t) = b$, then
$$\sigma_i(t + 1) = -m. \tag{1}$$
2. An automaton in any other active state, or in a refractory state has a spontaneous transition that is independent of its neighbor(s). Thus, if $1 \leq \sigma_i(t) \leq b - 1$, or $-m \leq \sigma_i(t) < 0$, then
$$\sigma_i(t + 1) = \sigma_i(t) + 1. \tag{2}$$

3. The communication between nodes is meant to mimic gap junctional coupling between neurons. In the biological situation, current flows directly between any two neurons that are connected by a gap junction, affecting the membrane potential of both. Depending on the number of gap junctional connections an individual neuron has to others, input from any of its neighbors may or may not allow the cell to become active [25]. This is taken into consideration by allowing a silent node to become active if there is an adequate input from its neighbors determined by a so called loading rule. In the case of simple loading (SL), a silent node becomes active at the next time step when it has at least one active neighbor. Through the majority rule (MR) a silent node can become active only if at least half of its neighbors are active. When considering small networks of nodes, we shall also utilize an absolute majority (AM) rule in which case more than half of the neighbors of a silent node must be active. Thus if $\sigma_i(t) = 0$, then,

$$\sigma_i(t+1) = 1 \text{ under } \begin{cases} \text{(SL) if at least one neighbor is active,} \\ \text{(MR) if at least half the neighbors are active,} \\ \text{(AM) if more than half the neighbors are active.} \end{cases} \tag{3}$$

As $N \to \infty$, there is no qualitative difference between MR and AM.

The configuration of the system at any time $t$ is specified by the vector $\sigma(t) = \{\sigma_1(t), \sigma_2(t), \ldots, \sigma_N(t)\}$. A periodic orbit is defined by the condition $\sigma(t+q) = \sigma(t)$ for some $q > 0$. A period-1 orbit is a fixed point, namely $\sigma(t+1) = \sigma(t)$, and as can be trivially seen, the unique fixed point of the system is $\sigma = 0$. In the present system, it is clear that all orbits are either eventually fixed or periodic since the state space of the system of $N$ nodes is finite, having size $r^N$.

We define the activity $A_f$ as the probability that an arbitrary initial condition lies within the basin of attraction of a periodic orbit. We are interested in determining how $A_f$ depends on the specific graph structure, intrinsic dynamics and nodal interaction rules within the network. The basic structure of a random graph as a function of edge probability was first investigated by Erdős and Rényi [14]. They showed that as the edge probability increases, different topological properties emerge at specific thresholds. Important for the present study are the phase transitions for an almost sure occurrence of an edge between two nodes at $p \sim O(1/N^2)$, of a cycle when $p \sim O(1/N)$ and for the disappearance of the last isolated node at $p \sim O((\ln N)/N)$. As discussed below, we have previously [17] related these thresholds to specific transitions of $A_f$ in the context of homogeneous networks. Our goal here is to relate these structural features to heterogeneous networks.

## 3. Dynamics on homogeneous networks

We briefly review a few of the key results from our previous work on homogeneous networks [17]. We have shown that under certain conditions $A_f$ undergoes a sharp transition from 0 to 1 around $p \sim O(1/N^2)$ for bursting neurons when $r \leq 2b$ and $r = b + 2$ with either the SL or MR interaction rule. The emergence of the first edge in the graph around $O(1/N^2)$ is a necessary condition for sustained periodic activity in bursting nodes. The condition $r \leq 2b$ ensures that nodes spend a sufficient amount of time in the active states to allow their effect to ultimately be felt by other nodes that are transitioning through the refractory states to the silent state. For example, when $r = b + 2$, as $b \to \infty$, the probability that a randomly chosen initial condition lies in the basin of attraction of a periodic orbit tends to 1 as increasingly more number of nodes are likely to be in the active state. We proved this result for the SL interaction rule in [17] and showed that it numerically holds in the MR case too. The reason for the latter is that when $p \sim O(1/N^2)$, the graph is dominated by sets of nodes connected by only a few edges. Thus, at this level of connectivity the effect of the SL and MR loading rules is identical in the network. The phase transition in $A_f$ for networks of spiking neurons ($b = 1$) that utilize the SL interaction rule occurs for $p \sim O(1/N)$ with the emergence of cycles. With the SL rule, the activity curves $A_f$ in these cases are a monotone increasing function of $p$.

When considering the MR rule for bursting nodes with $r \leq 2b$, we found in simulations that the shape of the activity curve $A_f$ is dependent on the fraction $f = b/r$. In [17], we conjectured that in the limit of $N \to \infty$, there exists a critical value, $f^*$ such that if nodes in the network have $1/2 \leq f < f^*$, the activity curve is a non-monotonic function of $p$. The local minimum of $A_f$ occurs around $O((\ln N)/N)$. If, however, $f > f^*$ then $A_f$ is monotone increasing under the MR rule. We provided some analytic justification for the conjectured existence of a critical fraction, which we estimated to lie in $12/19 < f^* < 7/11$. Below, we provide more analytic results to support the conjecture.

### 3.1. Networks of three nodes

A fair amount can be learned about how the loading rules affect activity in larger sized networks by building off of insights obtained from small network motifs. Indeed in our previous work [17], the emergence of a threshold at $p \sim O(1/N^2)$ for the activity of bursting nodes can be discerned from an analytic result we proved there for just $N = 2$ nodes. Here, we study the case of $N = 3$ homogeneous nodes to gain insight into the conjectured existence of $f^*$. For $N = 3$, the SL and MR rules affect network activity in identical ways. This is because a silent node can have at most two neighbors and both SL and MR require that at least one of the neighbors be in the active state for the silent node to become active. However, the AM rule differs, in that both neighboring nodes would need to be active for the transition $0 \to 1$ to occur. The result below utilizing the AM rule shows how non-monotonicity can arise as a function of edge probability $p$.

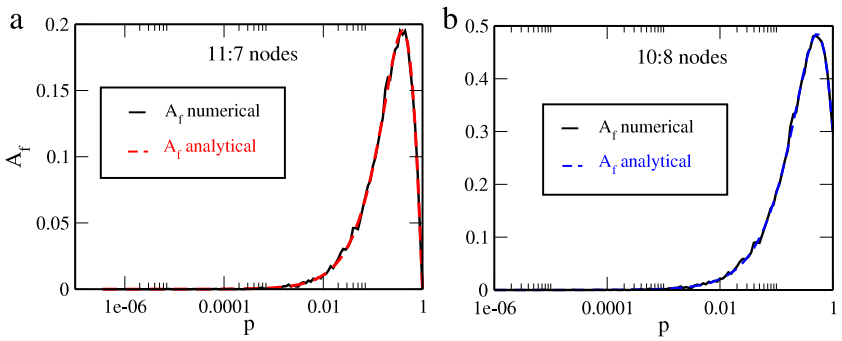


**Fig. 1.** Analytical (dashed lines) and numerical (solid lines) activity curves ($A_f$) for $N = 3$ nodes for different $r : b$ values (a) 11:7 and (b) 10:8. Note that in (a) since $f = 7/11$ is less than $2/3$, $A_f(p) \to 0$ as $p \to 1$. Numerical results were generated using the AM loading rule.

**Proposition 1.** *Consider the AM rule on a network of three $r : b$ nodes with $r = b + m + 1$ such that $r \leq 2b$. Then*

$$A_f(p) = 3p\,(1-p)\left(f - \frac{m}{r}\right)\left(1 - p + \left(f - \frac{m}{r}\right)p\right) + p^3\left(f - \frac{2m}{r}\right)\left(f - \frac{2m+1}{r}\right). \tag{4}$$

**Proof.** The activity on the random graph is equal to a sum over the product of the probability of a particular graph existing with the probability of activity existing on that graph. For the case of three nodes, there is one graph with no edges, three graphs with one edge, three graphs with two edges (like a $V$ shape) and one graph with three edges (a triangle). We denote the probability for activity to exist on any one of these subgraphs as $A_\emptyset$, $A_E$, $A_V$ and $A_\Delta$ respectively. Then as a function of edge probability $p$

$$A_f(p) = (1-p)^3 A_\emptyset + 3p(1-p)^2 A_E + 3p^2(1-p)A_V + p^3 A_\Delta. \tag{5}$$

Clearly $A_\emptyset = 0$. The prefactor of three on the second and third terms, comes from the three different ways in which each of these type of graph can be generated. Calculating $A_E$, $A_V$ and $A_\Delta$ depends on determining sets of initial conditions that are sufficiently spaced apart to guarantee that at any moment in time, a sufficient number of nodes are active. For the case of an edge, $A_E = (b-m)/r$. The easiest way to see this is to consider one of the nodes starting at the value 0. In order for this node to become active, the other node must already be active. However, its initial value must be greater than $m$, since if not, then both nodes would, at a future time, simultaneously be in the refractory or silent state. There are $r$ possible initial states of the second node, $m+1$ of these are refractory and silent. Of the remaining $b$, only those with a value greater than $m$ can lead to activity, thus leaving $b - m$ possible initial states. For the case of a $V$, $A_V = (b-m)^2/r^2$. This represents the probability that when the vertex is at state 0, the other two nodes are both active and more than $m$ steps away from 0.

To calculate $A_\Delta$, note that at any time when one node is in state 0, the other two nodes must be active in order to sustain activity on the triangle. This means that the initial state of the three nodes must be separated by at least $b - m$ steps from each other. For example, if one node is at state 0, the second node at state $m + 1$, then the state of the third node must be at least at $2(m + 1)$, but could also be at any value up to $b$. In particular, this means that $4 : 2$ and $5 : 3$ nodes cannot support activity on a triangle since they do not have enough bursting states relative to refractory states. Running through all possibilities, including relevant permutations, it turns out

$$A_\Delta = 2\frac{(1 + 2 + \cdots + b - 2m - 1)r}{r^3},$$

which after cancellation sums to $(b - 2m)(b - 2m - 1)/r^2$. Substituting into Eq. (5) and replacing $f = b/r$ yields Eq. (4). ■

Fig. 1 shows close agreement between the graph of $A_f$ obtained analytically from Eq. (4) compared with that from numerical simulations. Several implications arise from Proposition 1. First, since $m \geq 1$, for there to be activity on a triangle, it must be that $b \geq 4$. In general, $b \geq 2(m + 1)$ but $m + 1 = r - b$. Substituting and rearranging yields $3b \geq 2r$ or $f \geq 2/3$. This is the first clue that the fraction $f = b/r$ can play a role in the monotonicity or non-monotonicity of $A_f(p)$. In particular, if $f < 2/3$ , then $A_f(1) = 0$, while if $f \geq 2/3$, then $A_f(1) > 0$. Second, it is straightforward to calculate $dA_f(p)/dp$. Doing so, one finds that for each $f$, $A_f(p)$ always has a local maximum for $p < 1$. Thus $A_f(p)$ is non-monotonic when $N = 3$. Moreover, for $m$ fixed, as $f \to 1$, $A_f(1) \to 1$. It is easy to show that in this limit, $A_f(p)$ is monotone increasing.

We considered the AM rule because it allowed us to use $N = 3$ which is the smallest possible graph for which a cycle exists. A result similar to Proposition 1 could be derived for the MR rule on a minimal network of four nodes to show non-monotonic dependence on $f$. We have done several numerical simulations (not shown) confirming this to be the case.

## 4. Dynamics on heterogeneous networks

We now explore how different types of heterogeneities affect the ability of a network to sustain activity. We shall begin by proving a simple but useful result for a network consisting of two nodes, that provides a valuable insight into larger network behavior. Then we conduct a numerical study of $N = 50$ nodes in which we add heterogeneity in varying degrees into either the intrinsic dynamics of the nodes, or in the nodal interaction rules.

### 4.1. Small network motifs

Two homogeneous $(r : b)$ nodes with a single edge can have a period $r$ solution if and only if $r \leq 2b$ [17]. When the number of active states of each neuron exceeds the number of silent and refractory states, then a single edge suffices to guarantee the existence of a periodic orbit. For nodes connecting heterogeneous automata, additional requirements need to be met in order to obtain periodic solutions. For example, consider a 4:2 node connected to a 5:3 node. Starting with the 4:2 node in the silent state, it is straightforward to check that there does not exist an initial state of the 5:3 node that will lead to periodic activity. However, if a 4:2 node is connected to a 8:6 node, then the initial state $(0, 2)$ returns to itself after 8 steps as does the initial state $(0, 6)$. In part, this is because eight is multiple of four, but not five. However, a check of whether an edge between a 4:2 node and a 8:5 node supports periodic behavior shows that it cannot. In this case, the refractory length of $m = 2$ of the 8:5 node is equal to the burst length $b = 2$ of the 4:2 node and is too long to allow activity to be sustained. Thus, for periodic activity to exist between a pair of nodes, two requirements must be met: the total number of states of each of these must be multiples of one another and the refractory state of either of the nodes should not be too long compared to the bursting state of the other node. For this network of only two nodes, there are no transients leading to a periodic orbit. Namely, every initial state that converges to a periodic orbit lies on the orbit itself. This fact will allow us to calculate $A_f$. These observations are generalized in the following result.

**Proposition 2.** *Consider an $(r_1 : b_1)$ node connected by an edge to an $(r_2 : b_2)$ node, with $r_2 > r_1$ and $m_i = r_i - b_i - 1$, $i = 1, 2$. Then a period $r_2$ solution exists if and only if $r_2 = nr_1$, where $n$ is an integer and $m_2 < b_1$ under any of the loading rules. When these conditions are met and a periodic orbit exists, $A_f = (b_1 - m_2)/r_1$.*

**Proof.** In the case of two connected nodes, the effect of SL, MR and AM loading rules is equivalent. First assume $r_2 = nr_1$ and $m_2 < b_1$. Consider the initial condition $(0, b_2)$. The length of the refractory state for node 2 is $m_2$. After $m_2 + 1$ time steps, node 2 is in state 0, while node 1 is in a state $m_2 + 1 < b_1 + 1$. Thus $m_2 + 1 \leq b_1$ which implies that node 1 is still active. Therefore it can pass activity to node 2 at the next time step. After another $b_2$ steps node 2 reverts to $b_2$ while node 1 is in the state $m_2 + 1 + b_2 = r_2 = nr_1 = 0$. So the new state of the network is $(0, b_2)$ implying the existence of a period $r_2$ solution.

Note that if $m_2 \geq b_1$ then the initial condition $(0, b_2)$ does not lead to a periodic solution. After $m_2 + 1$ time steps, node 2 is in state 0, while node 1 is in a state $m_2 + 1 \geq b_1 + 1 > b_1$ which being an inactive state cannot pass activity to node 2 at the next time step. Similar analysis can be shown for any other initial state as well.

Next assume there exists a period $r_2$ solution. For any initial condition $(i, j)$, the minimum time steps required for the solution to return to $(i, j)$ will be the lowest common multiple (LCM) of $r_1$ and $r_2$. Since a period $r_2$ solution exists, hence LCM $(r_1, r_2) = r_2$. So we can conclude $r_2 = nr_1$, where $n$ is an integer.

Next consider an initial condition $(h, b_2)$. This state after $m_2 + 1$ time steps becomes $(h + m_2 + 1, 0)$. Since a periodic solution exists, so in order that the activity is passed from node 1 to node 2 which is now in 0 state, the former should be in one of its active states, namely, $1 \leq h + m_2 + 1 \leq b_1$. So, $-h \leq m_2 \leq b_1 - 1 - h$ leading to $m_2 < b_1$. This can be worked out for any other initial condition as well.

To calculate the fraction of initial states that lie on a periodic orbit, note the following. First, the size of the state space is now $r_1 r_2$ and the length of a periodic solution will be $r_2$. Next, start with the $(r_2 : b_2)$ node at state $-m_2$. Clearly the other node must already be active and must stay active for at least $m_2$ steps. The difference $b_1 - m_2$ provides the number of initial states that this node can be in, for activity to persist. Thus, $A_f = r_2(b_1 - m_2)/r_1 r_2$, which after cancellation yields $A_f = (b_1 - m_2)/r_1$. Note, that this formula reduces to $A_E(p)$ computed in Proposition 1 for homogeneous nodes. ■

Activity continues to be sustained with the addition of a new node to an edge of the above types, namely between two $(r : b)$ nodes with $r \leq 2b$ or between $(r_1 : b_1)$ and $(r_2 : b_2)$ such that $r_2 = nr_1$ and $m_2 < b_1$, irrespective of its intrinsic dynamics. Even after the addition of a third node to the network, the SL and MR loading rules continue to be satisfied. These results suggest that the phase transitions at $O(1/N^2)$ and $O(1/N)$ observed for homogeneous networks [17] should, in certain contexts, continue to exist in the presence of heterogeneity.

Although Proposition 2 considers the case of only two nodes, its real use is in understanding the behavior at large $p$ in a larger network. For example, in a fully connected network at $p = 1$, our earlier work [17] shows that for a homogeneous network using MR, $A_f \to 1$ as $N \to \infty$ if $f > 0.5$. The proof of that result relies on a sufficient number of nodes being active at any time step. Now, in a heterogeneous network consisting of, say half 6:4 and half 7:5 nodes where $r_2 \neq nr_1$, the generalization of Proposition 2 would predict that for large $N$, $A_f \approx 0$ at $p = 1$, since seven is not a multiple of six. This is because a silent node would need at least half of the entire network to be active in order to become active. Thus the problem, to some extent, can be thought of as the entire population of 6:4 nodes connected with the entire population of 7:5 nodes. Proposition 1 then shows that the states of the active nodes must be sufficiently separated in order to maintain the AM rule,

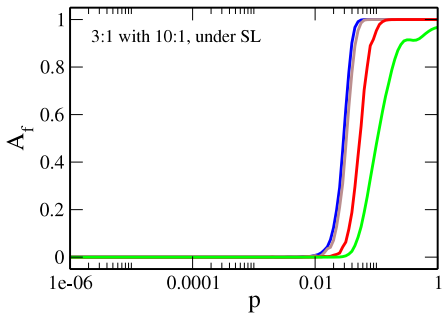


**Fig. 2.** Dynamics of heterogeneous ER networks ($N = 50$) with spiking nodes under the SL rule. Starting with a homogeneous $3:1$ network (blue curve), as the fraction of $(10:1)$ nodes increase in the network, the phase transition in activity curves $A_f$ occurs at larger $p$ values with the brown, red and green curves respectively showing dynamics with 10%, 50% and 90% $(10:1)$ nodes. Blue curve shows the activity in the homogeneous $3:1$ network under SL rule. (For interpretation of the references to color in this figure legend, the reader is referred to the web version of this article.)

thereby, placing a further constraint on the set of initial conditions that converge to a periodic solution. We shall study this case numerically in Section 4.2.1 below.

In turn, we can now see how our small network findings in the heterogeneous ($N = 2$) and homogeneous ($N = 3$) cases help to predict $A_f$ for all $p$ in larger networks for the MR case. Namely, for small values of $p$ of $O(1/N^2)$, the random graph is dominated by edges between two nodes. Thus, we would expect activity to emerge independent of the nature of heterogeneity, provided that some subset of nodes had $r \leq 2b$. As $p$ increases to $O(1/N)$ and larger, depending on the fractions $f_1$ and $f_2$ of the different nodes and based on the results of Proposition 1, we would expect to see a local maximum in $A_f$ occur as cycles arise. Finally, depending again on $f_1$ and $f_2$ and whether or not the conditions of Proposition 2 are met, we would predict either that $A_f \to 0$ or 1 as $N \to \infty$. The simulation results below will validate this intuition.

### 4.2. Networks

The results presented here are for simulations on heterogeneous networks of size $N = 50$ as a function of $p$. We partitioned the interval [0, 1] of probability values such that for values of $p$ close to $O(1/N^2)$ and $O(1/N)$, a finer partition was chosen. At each $p$, $10^4$ initial conditions are randomly chosen. Each of these is evolved on the graph under a certain interaction rule to obtain a steady state response of the network. $A_f$ is computed as the fraction of initial conditions that lead to periodic behavior. This is repeated for $2 \times 10^3$ graph realizations and an average value of $A_f$ is computed at each $p$. We adopt this methodology throughout this work unless it is specified otherwise. The global dynamical behavior of a binary mixture of neuronal automata on ER networks mainly differs from the homogeneous case on quantitative aspects: differences are found in terms of an increase in activity levels, a shift in emergence thresholds. Qualitative variations can be seen as changes in monotonicity properties as well as in the presence of non-zero dynamical activity in comparison to the corresponding homogeneous case. These findings are illustrated below.

#### 4.2.1. Heterogeneity in intrinsic nodal properties

Consider a network with a mixture of spiking nodes of different refractory lengths $m_1$ and $m_2$. For example, we take a network of (3:1) nodes under the SL rule (here, cycles are a pre-requisite for sustained activity) and replace a random fraction by (10:1) automata (such that, $m_1 < m_2$). The activity curves, shown in Fig. 2, undergo a transition to $A_f \to 1$ at increasing values of $p$ along with a gradual decrease in the activity levels as the proportion of (10:1) nodes increases in the network. This can be explained as follows: with increasing $p$, a higher number of longer length cycles are formed but the state space grows at a faster rate than the initial conditions that lead to sustained activity (most just go to the fixed point). However, this is a finite $N$ effect. In the limit as $N \to \infty$, the phase transition in $A_f$ occurs at $O(1/N)$. Under MR loading rules, isolated cycles are required for sustained dynamical activity. Minimal cycle (or isolated closed loops) appear for a vary narrow range of $p$ values around $O(1/N)$ [14] and are destroyed completely in the limit $p \to 1$. As shown earlier [17], for a homogeneous network of spiking neurons with MR, $A_f$ is close to 0 for all $p$ and the addition of heterogeneity does not affect this (simulations not shown).

Next, we couple nonidentical bursting nodes, $b_1 \neq b_2$ with $m = 1$ for both. We start with a network of $(10:8)$ $(f > f^*)$ nodes and replace a fraction with $5:3$ $(f < f^*)$ at random sites. Note, that this heterogeneous set of nodes satisfies Proposition 2. With the increase in the level of heterogeneity in the network, the phase transition in the $A_f$ curves to full activity occurs at increasing values of $p$ under the SL rule. Under the MR rule, heterogeneity changes the monotonicity properties of $A_f$. In particular, $A_f$ for a homogeneous network of $10:8$ nodes is monotone increasing since $f = 8/10 > f^*$, while $A_f$ for a homogeneous $5:3$ network is non-monotone since $f = 3/5 < f^*$. Thus as the proportion of $5:3$ nodes increases, there is a concurrent decrease in $A_f$, consequently, nonmonotonic behavior begins to set in and continues to become more pronounced as the network switches towards $5:3$ type (Fig. 3). We expect that these types of non-monotonic

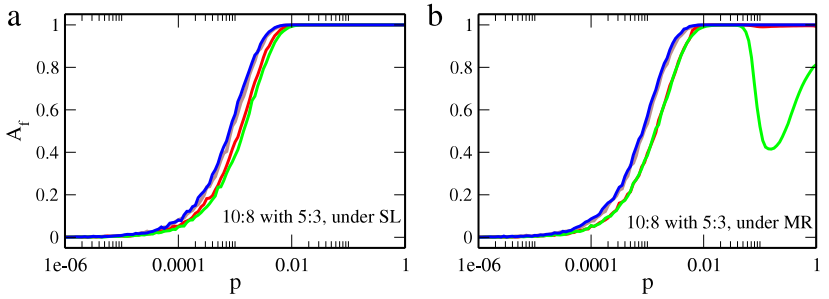


**Fig. 3.** Dynamics of heterogeneous ER networks ($N = 50$) with bursting nodes under the (a) SL and (b) MR rule. The green curve corresponds to a homogeneous $10 : 8$ network. The brown, red and green curves respectively show dynamics with 10%, 50% and 90% $5 : 3$ nodes. Blue curve is the homogeneous 10:8 curve under SL in (a) and under MR in (b). (For interpretation of the references to color in this figure legend, the reader is referred to the web version of this article.)

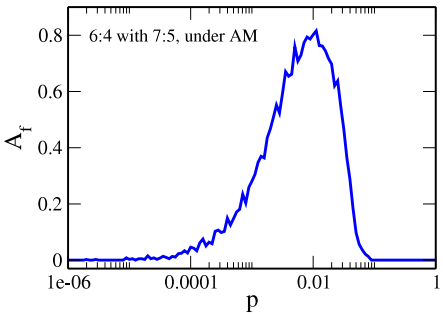


**Fig. 4.** Dynamics of heterogeneous ER networks ($N = 50$) with $6 : 4$ and $7 : 5$ bursting nodes distributed randomly in equal proportion (50% heterogeneity). The loading rule used in this graph is Absolute Majority (AM). The jaggedness in the curve is due to small ensemble averaging.

behaviors persist as $N \to \infty$. In that event, we expect the phase transition of $A_f$ from $1 \to 0$ occurs in the graph around $O(1/N)$ when the giant component begins to emerge, whereas, $A_f$ switching from $0 \to 1$ appears to be related to the disappearance of the last isolated node around $O(\ln N/N)$, consistent with our results in [17].

In Fig. 4, we show the case of $(6 : 4)$ and $(7 : 5)$ nodes interacting via the AM rule. Both sets of nodes obey $f \geq 1/2$ and additionally the conditions in Proposition 1. Thus, one would expect the activity $A_f$ to emerge at $O(1/N^2)$ as it does. But the pair does not satisfy the conditions of Proposition 2 since seven is not a multiple of 6. Therefore, we would expect a local maximum near $O(1/N)$ and that as $p \to 1$, $A_f \to 0$. This is exactly what happens. Near $O(1/N)$, activity in the network is supported on edges, V-like graphs and cycles. But as the graph becomes more connected, AM becomes increasingly more difficult to be satisfied.

Another possible network of heterogeneous nodal dynamics is where spiking and bursting nodes are distributed randomly on a network. To illustrate, we begin with a network of $4 : 1$ nodes and replace a fraction of them by $6 : 4$ ($f > f^*$) or $5 : 3$ ($f < f^*$) nodes. Spiking nodes need cycles (appearing at $O(1/N)$) while bursting nodes require edges emerging at $O(1/N^2)$ for sustained activity (monotonic for both) under SL [17]. As a result with the increase in the proportion of $6 : 4$ $(5 : 3)$ nodes in the network, the $A_f$ curves undergo a transition to the full activity level at lower values of $p$ (Figs. 5(a), 6(a)). Under MR, the emergent dynamics for identical bursting nodes coupled on a random ER network is either monotonic or nonmonotonic depending upon the value of the ratio $f$. On the other hand, the non monotonic dynamics of a pure spiking network is supported by minimal cycles which get destroyed as $p \to 1$ [17]. When the heterogeneous network is subjected to MR rule, as the number of bursting nodes increase in the network, we observe that the activity curves $A_f$ have small (nonzero) values in the limit $p \to 1$. Also, even at intermediate values of $p$, bursting nodes support more activity thus resulting in an overall increase in $A_f$ when significant number of sites in the network become of the bursting type (Fig. 5(b), Fig. 6(b)).

*4.2.2. Heterogeneity in nodal interaction rules*

Of the various cases of heterogeneity considered so far in this work, networks with mixed interaction rules turned out to be the most intriguing. We begin to understand their dynamics by considering first a network of identical spiking nodes interacting with each other through SL rule. Then an increasing fraction of sites are randomly made to interact via MR. When the network works simultaneously with both the rules, the transition point in the activity curves shifts to higher $p$ values and activity drops down as the proportion of nodes interacting via MR rule increases. This makes sense as now fewer nodes are able to participate in the oscillatory behavior. Provided there remain a sufficient number of nodes that use SL within the network, there is still some non-zero activity in the $p \to 1$ limit. In particular, for $r : 1$ nodes, as long as at least $r$ nodes

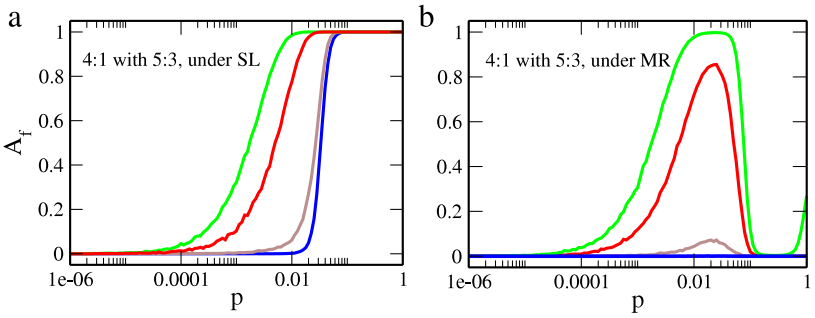


**Fig. 5.** Dynamics of ER networks ($N = 50$) with $4:1$ and $6:4$ ($f > f*$) nodes under the (a) SL and (b) MR rule. Different colors show different fractions of heterogeneity ($6:4$), namely, blue-0%, brown-10%, red-50%, and green-90%. (For interpretation of the references to color in this figure legend, the reader is referred to the web version of this article.)

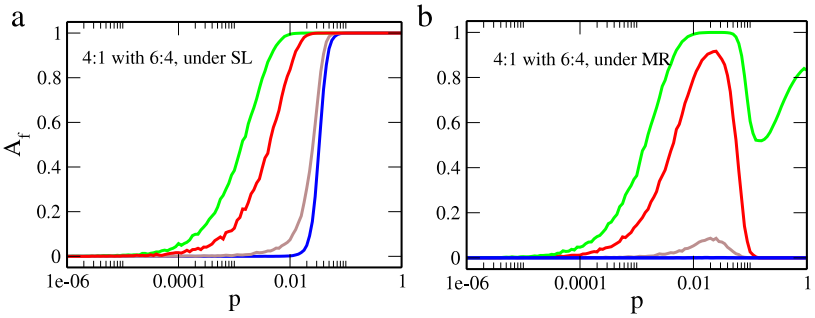


**Fig. 6.** Dynamics of ER networks ($N = 50$) with $4:1$ and $5:3$ ($f < f*$) nodes under the (a) SL and (b) MR rule. Different fractions of heterogeneity are shown with different colors, namely, blue-0%, brown-10%, red-50%, and green-90%. (For interpretation of the references to color in this figure legend, the reader is referred to the web version of this article.)

remain that utilize SL, $A_f \neq 0$ at $p = 1$. To illustrate this case, we show the example of $3:1$ ($10:1$) nodes connected on a network and interacting via both the excitation rules simultaneously. Note at 90% heterogeneity (green curve), there are still 5 nodes that utilize SL, therefore, in Fig. 7(a), the activity curve for $3:1$ nodes has a non-zero value at $p = 1$, while it is zero for $10:1$ nodes (Fig. 7(b)).

When bursting nodes interact via both these excitation rules concurrently, we observe that there is not much shift in the activity curves with the increase in the number of MR obeying nodes in the network. We show results for $4:2$ ($f < f*$) as well as $6:4$ ($f > f*$) nodes in Fig. 8. For $6:4$ nodes we have just one monotonic curve for all levels of heterogeneity while for $4:2$ nodes we have overlapping curves with $A_f \to 1$ at full connectivity. This is in sharp contrast to the behavior observed in the homogeneous case, wherein, at low values of $p$, activity curves for $4:2$ nodes under SL and MR overlap, but as $p \to 1$, nonmonotonicity sets in the MR curves and $A_f \to 0$ at $p = 1$ [17].

Near $p = 1$, when the fraction of nodes obeying MR increases in the network, the transient time needed to reach the periodic solutions also increases. Once these transients die out, all the nodes satisfying the MR become silent and they stop contributing to the evolution of the state vector. On the remaining fraction of nodes which satisfy the SL rule, all initial conditions lead to sustained activity. Thus, even when large numbers of nodes in the network are interacting via the majority rule, effectively it behaves as a network of a smaller size operating only under the SL rule. Further, we calculated the average number of active sites present in the network at any time for $p = 1$, at different levels of heterogeneity, for $3:1$ and $4:2$ nodes. Our numerical simulations show that for 3:1 automata, at any level of heterogeneity, the average number of active sites is essentially 1/3 of the number of nodes that use SL since each $3:1$ automaton will on an average be active for one-third of the time. For 4:2 nodes, the number of active sites at any time for all levels of heterogeneity is on an average half of the total number of nodes using SL. This behavior of the dynamical activity curves is also recovered if we start with a network of nodes operating via MR and then at a random fraction of sites interaction rule is gradually changed to SL.

*4.2.3. Heterogeneity at nodes of higher degree*

Until now, our focus has been to study the effect of different types of heterogeneities placed on random sites of an ER network. As the probability of having an edge $p$ increases gradually from 0 to 1, the nodes in the graph pick up connections, their degree increases and as a result the network grows from being sparse to being fully connected. Further, in the limit $N \to \infty$, the average degree of all the nodes in an ER graph converges to $Np$, however, this result does not hold true for the finite size random graphs that we deal with in this work. Indeed, as edges grow with increasing $p$, some nodes acquire

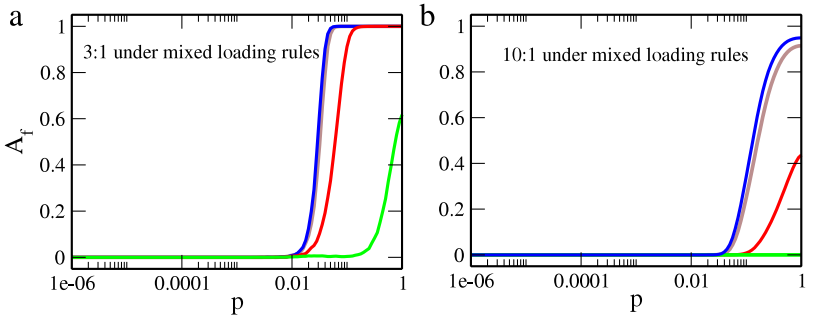


**Fig. 7.** Spiking nodes on a ER network: (a) (3 : 1) and (b) (10 : 1), on a network of size $N = 50$, under a mixture of SL and MR rules. Here different colors denote different fraction of nodes obeying the MR rule, namely, blue-0%, brown-10%, red-50%, and green-90%. (For interpretation of the references to color in this figure legend, the reader is referred to the web version of this article.)

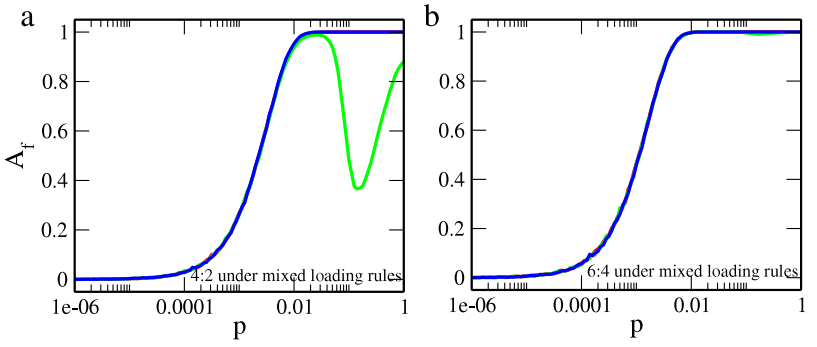


**Fig. 8.** Bursting nodes on a ER network: (a) (4 : 2) and (b) (6 : 4), on a network of size $N = 50$, under SL and MR rules.

higher degrees than others. In prior sections, since we placed the heterogeneities randomly in the network, there was an equal chance of these occurring at nodes of lesser or higher degree. To understand the impact of higher degree nodes on network dynamics, we now occupy such nodes with the various forms of heterogeneities considered above.

In Fig. 9(a), we show how the degree distribution of the nodes of the highest five degrees changes as the edge probability $p$ increases, calculated for an ensemble of $10^4$ random graphs. The $y$ axis in these figures shows the number of nodes of different degrees (largest, second largest and so on). As expected, at lower values of $p$ very few nodes have edges, while most nodes remain isolated. Note the black curve emerges around $O(1/N^2)$ consistent with the phase transition that occurs with the emergence of the first edge. As the graph grows, the largest set of nodes are those with the second (red), third (green), fourth (blue), fifth (magenta) and sixth (brown) highest degrees. The graph becomes connected at $O(\ln N/N)$ from which point on the number of nodes of varying degree starts to even out. Fig. 9(b) shows a cumulative growth of the nodes shown in Fig. 9(a).

Fig. 10 shows $A_f$ in the situation where the graph started with 4 : 1 spiking dynamics and we gradually replaced these with 5 : 3 bursting dynamics at nodes of increased degree. We can compare these graphs with Fig. 6 in which the replacement of 4 : 1 nodes with 5 : 3 nodes occurs at random sites. In panel (a), using the SL rule, only four curves (black, red, green and the remaining overlapping in brown) are visible. Note that the activity here emerges at $O(1/N^2)$ which is in contrast to Fig. 6a, where the activity emerges at $O(1/N)$ (blue curve) for the homogeneous case. This makes sense because 5 : 3 nodes can sustain activity with a single edge, whereas 4 : 1 nodes require cycles. Thus by placing the heterogeneity specifically at a site with higher degree, the graph begins to exhibit sustained activity at lower edge connection probability. Further, it also shows that the activity in the network is almost entirely driven by the sets of nodes with the two highest degrees, a result that cannot be discerned from Fig. 6a. Fig. 10b shows results when the MR rule is utilized. Here again the emergence of activity is at $O(1/N^2)$, however, in contrast to the SL rule, the activity is not restricted to the sets of nodes with the two highest degrees, but relies on nodes of all degrees.

Next, we generate activity curves with spiking nodes using the majority rule at sites with higher degree while SL rule operates on the other nodes. In Fig. 11(a), we see that the transition point in $A_f$ shifts to higher $p$ values when heterogeneity is increased at high degree nodes, but the shift here is more gradual and the activity levels are also higher when compared to Fig. 7(a). This can be understood by considering Fig. 9(b). Note that at large $p \in (0.1, 0.8)$, only about 20 or so nodes (brown curve) are the ones at which MR is operating. The remaining 30 or so nodes still use SL, for which 3 : 1 nodes can sustain activity, and therefore $A_f$ remains large. When the nodes are of 10 : 1 kind instead, Fig. 11(b), the dynamical curves are

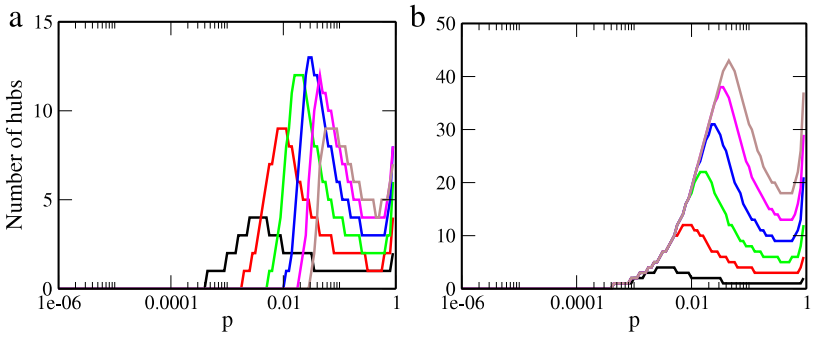


**Fig. 9.** Growth in the number of high degree nodes with edge probability $p$ for $N$ =50. Nodes with largest degree are shown in black, followed by nodes of lower degree in red, green, blue, magenta, and brown, respectively. (a) The non-cumulative number of higher degree nodes (b) The cumulative growth. (For interpretation of the references to color in this figure legend, the reader is referred to the web version of this article.)

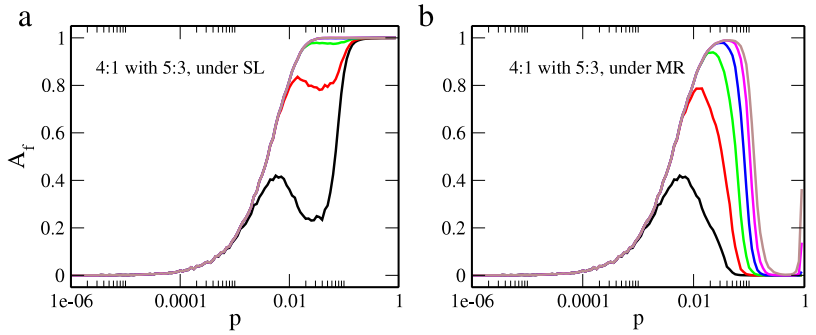


**Fig. 10.** Dynamics of ER networks ($N = 50$) of $4 : 1$ nodes with $5 : 3$ at higher degree nodes. Color scheme as in Fig. 9. Activity emerges at $O(1/N^2)$ (a) Under SL, activity is driven by the sets of nodes of the two highest degree. (b) Under MR, activity is driven by all nodes. (For interpretation of the references to color in this figure legend, the reader is referred to the web version of this article.)

further shifted to higher $p$ values when compared to panel (a), but the activity largely persists in contrast to Fig. 7(b), due to similar reasons as stated above, however, it does converge to 0 as $p \to 1$.

There are situations where introducing heterogeneity at higher degree nodes yields no qualitative difference from cases where the same heterogeneity was introduced at random. For example, Fig. 12 shows results for $10 : 8$ and $5 : 3$ nodes that is to be compared with Fig. 3. Under SL, the activity curves in panel (a) of each figure are qualitatively the same. This is because both $10 : 8$ and $5 : 3$ are bursting nodes, so wherever they appear in the graph, a single edge is sufficient to sustain activity. Similarly, under MR, Fig. 12b shows that as more nodes use $5 : 3$, $A_f$ becomes non-monotonic (brown curve for example), consistent with Fig. 3b (green curve).

Together, these results show that restricting heterogeneity to higher degree nodes can increase the chance of the graph to sustain activity. Whether it does or not depends on the type of heterogeneity introduced and the type of loading rule used for the interactions.

### *4.3. Boolean Lyapunov exponent and the semi-annealed process*

The random networks discussed in this work are quenched systems, namely, once the graph is generated at a certain $p$ value and the dynamical update rule is chosen, these remain fixed throughout the evolution of dynamics on these graphs (quenched randomness). The dynamics ($A_f$) undergoes phase transitions at critical points which are closely related to emergence of certain structural features in the architecture. For doing a stability analysis in such graphs, Derrida and Pomeau proposed an "annealed" approximation [22] and modification of the same by Pomerance et al. [20] lead to a "semi-annealed" approximation. In the former, random choices of network edges and update rules are made at every time step. In the latter, while the architecture is fixed, only the update rules are randomly picked up at every time step. Two nearby initial conditions are co-evolved in an annealed (semi-annealed) system, whether their mutual separation grows or decreases with time determines the stability of the underlying system. The hypothesis is that the stability of an annealed (semi-annealed) system, which can be computed analytically, is a good approximation for the stability of the related quenched network [22]. The Boolean Lyapunov exponent (BLE) $\Lambda$ [24], a measure based on these approximations provides a useful characterization of the dynamics. This measure of the rate of separation of two nearby orbits is defined as follows [26]. A reference state of length $N$ is perturbed randomly to create a new state vector, and these states are then evolved simultaneously for a finite number

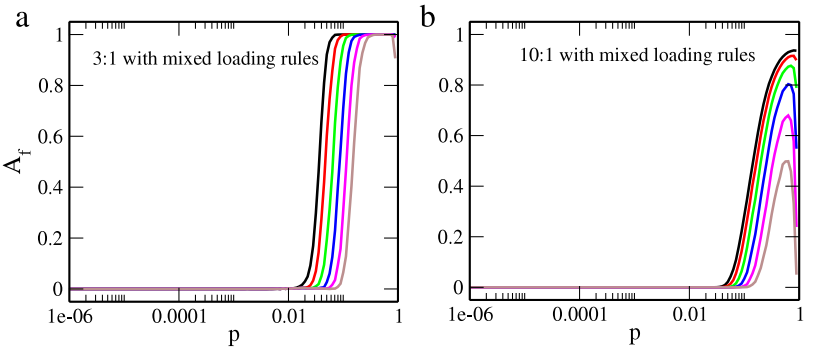


**Fig. 11.** Dynamics of ER networks ($N = 50$) of (a) $3:1$ nodes and (b) $10:1$ nodes, operating under mixed loading rules with nodes using MR at higher degree nodes and SL at the others. Color scheme as in Fig. 9. $A_f$ remains bounded away from 0 over a range of $p \in (0.1, 0.8)$ because a large number of nodes continue to use SL. (For interpretation of the references to color in this figure legend, the reader is referred to the web version of this article.)

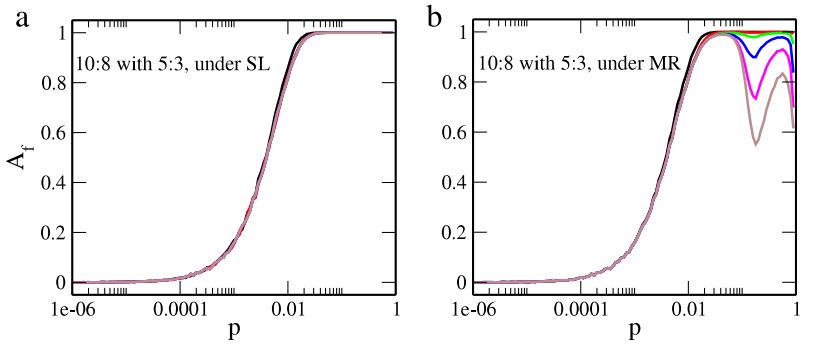


**Fig. 12.** Dynamics of ER networks ($N = 50$) of $10:8$ nodes with $5:3$ at higher degree nodes, under (a) SL and (b) MR. Color scheme as in Fig. 7. (For interpretation of the references to color in this figure legend, the reader is referred to the web version of this article.)

of steps $T$, their initial and final Hamming distances being denoted $d_{in}$ and $d_{out}$ respectively. For the $k$th such perturbation, the rate of divergence, $\lambda_k$, is

$$\lambda_k = \frac{1}{T} \ln \frac{d_{out_k}}{d_{in_k}}. \tag{6}$$

The Boolean Lyapunov exponent is obtained as an average rate of expansion over a large number of realizations,

$$\Lambda = \langle \lambda_i \rangle. \tag{7}$$

Both $\Lambda$ and the activity curves $A_f$ have the same functional dependence on $p$ for homogeneous or heterogeneous networks under both interaction rules; results are presented in Fig. 13. This can be understood as follows. Consider a homogeneous network of spiking $r:1$ nodes under the SL rule with $N$ sufficiently large. If $p$ is small, then $A_f$ = 0. To compute $\lambda_i$ for this case, any trajectory, including the reference trajectory, should converge to the fixed point $\sigma = 0$. Thus $d_{out_i} = 0$, we define $\lambda_i = -50$ for this case. Thus $\Lambda$ is proportional to some predefined negative number if $p$ is sufficiently small. Alternatively, when $p = 1$ and the graph is complete, we know that the basin of attraction of any periodic orbit is precisely the orbit itself [17], namely, there are no transients when approaching a periodic solution. Now, if we consider a reference trajectory that lies on a periodic orbit, a perturbation $i$ of this trajectory of size $d_{in_i}$ can lead to two possibilities: (a) it will lie on a different periodic orbit (including a translation of the reference trajectory). In this case, because there are no transients, $d_{out_i} = d_{in_i}$. Therefore, $\lambda_i = 0$. (b) The perturbation will lie on a trajectory that converges to the fixed point $\sigma = 0$. In this case, $d_{out_i} \geq r - 1$. Thus, $\frac{1}{T} \ln \frac{(r-1)}{d_{in_i}} \leq \lambda_i < 0$, hence, giving a lower bound to BLE. As $N$ grows increasingly, the phase space of initial conditions lying in the basin of attraction of $\sigma = 0$ decreases, thereby, reducing the likelihood of a negative contribution of $\lambda_i$ to the BLE. This implies that for $N$ large enough, at $p = 1$ for spiking nodes with SL interaction rules, $\Lambda = 0$. However, this explanation does not provide a rationale for the phase transition that the BLE undergoes around $O(1/N)$, but it is not unreasonable to expect the BLE to be a monotone increasing function of $p$ as more and more initial conditions fall out of the basin of attraction of $\sigma = 0$.

In Fig. 14, we present numerical calculations of the Hamming separation between two co-evolving initial conditions on a homogeneous random graph using a semi-annealed approximation. For these simulations, at an edge connection probability

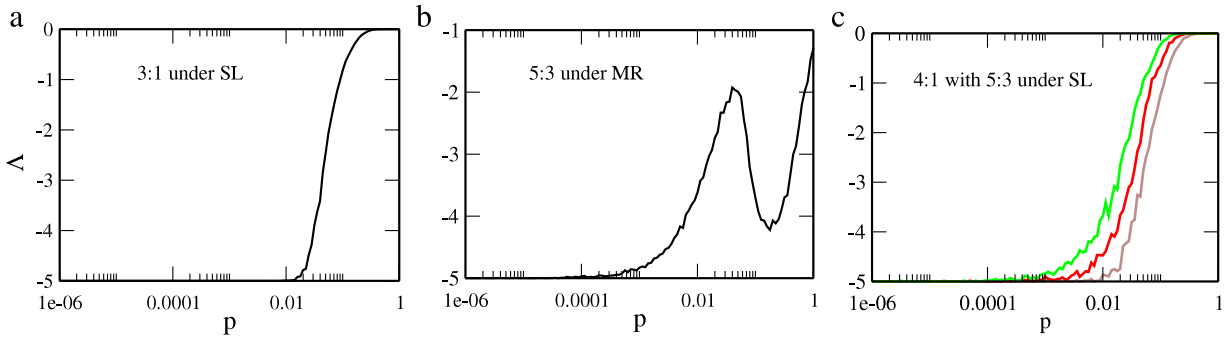


**Fig. 13.** Boolean Lyapunov exponent as a function of $p$ for homogeneous and heterogeneous ER networks. Ensemble size: 50 graphs and 50 initial conditions. (a) and (b) show $\Lambda$ vs. $p$ behavior for homogeneous $3:1$ and $5:3$ networks under SL and MR respectively while (c) captures this behavior for $4:1$ network under SL rule with brown-10%, red-50%, and green-90% nodes occupied by $5:3$ heterogeneity. (For interpretation of the references to color in this figure legend, the reader is referred to the web version of this article.)

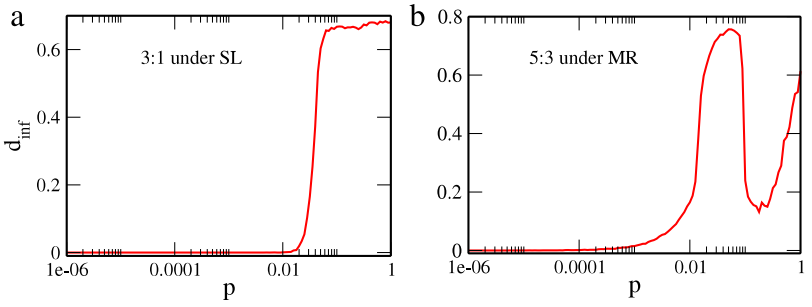


**Fig. 14.** Semi-annealed Approximation: Hamming distance between two co-evolving trajectories (averaged over 500 reference trajectories) as a function of $p$ for homogeneous automata networks of size $N = 50$: (a) $3:1$ nodes under SL and (b) $5:3$ nodes under MR.

$p$, the intrinsic dynamics of the node as well as the interaction rule are fixed. We start with two initial conditions, one being the reference trajectory. At each time step $i$, we generated a new random graph and evolved the existing state of the two vectors for one step, followed by calculation of their Hamming distance ($d_i$) normalized by the number of nodes, before repeating the process. This algorithm is repeated over several time steps and we arrive at the quantity $d_{inf}$. An ensemble average is computed over a number of reference trajectories and the entire process is repeated for each $p \in [0, 1]$. As can be seen, this semi-annealed approximation produces graphs that are qualitatively similar in shape and have phase transitions at similar orders of $p$ as both the BLE (Fig. 13(a) and (b)) and activity curves $A_f$ [17]. This suggests that some analytic headway may be achieved in calculating $A_f$ for large networks using techniques from [20,21].

While the BLE ($\Lambda$), the semi-annealed approximation ($d_{inf}$) and $A_f$ look similar, the manner in which we make their computations is different. The activity $A_f$ measures the size of the subset of the state space that converges to nontrivial periodic solutions. As such, it measures the long term behavior of an individual trajectory. The BLE, on the other hand, compares a short term behavior of nearby trajectories in order to predict the asymptotic dynamics displayed by the system. It calculates how quickly two nearby trajectories converge or diverge from one another, thus often used as a measure to detect the presence of chaos, which is surely not a feature of the finite size state space models considered here. Finally, the semi-annealed approximation calculation measures short-term divergence or convergence under the assumption that the network is following the average behavior of trajectories at each time step. Despite the differences in how these three measures are calculated, they appear to convey similar information. We do note, however, that calculation of the BLE is computationally more expensive as more sample trajectories are needed to calculate average behavior. Similarly, the semi-annealed approximation requires the generation of a new random graph at each time step adding to its computational cost. Here, we compensate by averaging over a smaller ensemble size, despite which fairly smooth transition curves are obtained (see Figs. 13 and 14 ).

## 5. Results and discussion

Heterogeneous networks of interacting automata [27–29] share many of the dynamical features of the homogeneous case. In particular, structural features and motifs of the network are closely related to phase transitions in the dynamical activity: the thresholds for the emergence of the first edge (for $p \sim O(1/N^2)$), cycles (for $p \sim O(1/N)$) and for the disappearance of the last isolated node ($p \sim O((\ln N)/N)$) demarcate various phase transitions in sustained activity $A_f$.

The discrete dynamics studied in this paper trace their origins to study of Random Boolean Networks of Kauffman [8]. Furthermore, the specific nodal interaction rules one could consider on such a network are addressed in a large body of literature. For example, our SL interaction rule can be found in the earlier work of Greenberg and Hastings [30], where the authors study lattice dynamics for nodes coupled by nearest neighbor interactions. They were interested in finding spatially inhomogeneous solutions, in particular, spiral waves of activity on the graph. They show how to identify a small network motif, in terms of initial values on the graph, that lead to spiral waves. The other interaction rule that we use, MR, is closely related to the voter model studied by Moore [31] where the state of each node is determined by majority vote of its neighbors. Moore showed that for a restricted set of initial conditions, the voter model is equivalent to calculating the probability of a transition in a zero-temperature Ising model. The main interest in this paper is to quantify whether it is possible to compute the asymptotic behavior of the model any faster than through direct simulation. While the emphasis of Moore's work is on solving a theoretical problem in computer science, the parallels to our work are worth noting.

The introduction of heterogeneity affects the thresholds that are relevant under different circumstances, and can be used to reduce the functional number of nodes that are able to participate in a specific dynamical activity. For example, when both the SL and MR loading rules operate, and the graph becomes more connected (as $p$ increases) only those nodes that interact through the SL rule can participate in periodic activity; all other nodes eventually become silent. In a biological context, this is a type of plasticity whereby connections between neurons weaken when they are not simultaneously active. While this type of plasticity occurs in Hebbian synaptic connections [32], it is also postulated to occur in networks of developing neurons coupled by gap junctions [33].

Heterogeneity can also increase activity $A_f$ so that the transition occurs at $p \sim O(1/N^2)$ rather than $O(1/N)$ if the heterogeneous node has higher degree; this can provide insight into how larger scale-free networks [15] of neurons might behave. Analyzing phase transitions in networks with discrete nodal dynamics has received considerable attention [21,34]. To this end, several techniques can be found in the literature. In particular, we make use of the Boolean Lyapunov exponent and numerical evidence suggests that the shape of activity curve $A_f$ along with its accompanying phase transitions can be inferred from the Boolean Lyapunov exponent. This observation could be found useful while analyzing data from other cellular automata models [35,36]. The roots of the BLE can be found in the works of Derrida et al. [22,23]. It is built upon the annealed approximation, wherein, instead of working with the quenched network, annealed configurations related to the system are generated to capture the critical points in the model. Much of the analytic work done in the semi-annealed approximation is on tree-like graphs [21] or for those that can be described using a threshold contact process [37]. The critical points in the activity curve $A_f$ in our network are related to emergence of certain structural features, which are well established in the literature of random graphs [14]. It is of interest, and remains an open problem, to analytically approximate the shape and phase transitions in $A_f$. The annealed and semi-annealed approximations represent one possible avenue to do so.

Several other studies focus on the relationship between topology and emergent dynamics for cellular automata networks. In particular, Larremore et al. [38] study the impact of heterogeneity in nodal dynamics on network response. In contrast to our deterministic update rules, their work deals with a probabilistic model, wherein the dynamics and architecture are coupled through the elements of the adjacency matrix ($A_{ij} \in [0, 1]$), which appear in the update rules from silent to excited state. The largest eigenvalue of $A_{ij}$ serves as an order parameter to detect the transition from subcritical (a quiescent network) to supercritical regime (a network is self-sustained activity). Similar to our work, the authors consider heterogeneities in the refractory period of nodes. They find that if the number of refractory states is increased in a correlated manner, then the level of activity in the graph is likely to decrease. Our work is consistent with this finding where we showed that both the bound $f \geq 1/2$ for the fraction of bursting states, and the ratios $f_1$ and $f_2$ of the heterogeneous nodes plays a role in determining network dynamics. In our case, it is not just that an increase in the duration of the refractory state may change the dynamics, but it is also a function of the specifics of how $f_1$ changes relative to $f_2$.

Neuronal networks in nature are intrinsically heterogeneous, with individual neurons having the capability of firing at frequencies that range from very slow (0.5 to 4 Hz [39]) to very fast (∼200 Hz and beyond [40]) oscillations. Some neurons are not intrinsically active but are excitable. The connection between the geometry of the heterogeneous neuronal network and its ability to sustain activity has been explored in the present work. It would be interesting to examine whether the inclusion of inhibition permits activity to be sustained; in a related model [41] it was shown that inhibition can create sustained activity in otherwise quiescent excitable systems.

Neurons with different types of intrinsic properties often interact within the same neuronal network [42]. From the modeling perspective, the introduction of oscillatory, rather than excitable nodes, is another form of heterogeneity to consider. Doing so would then allow us to study a network's ability to sustain oscillations as a competition between the drive provided by the oscillatory nodes compared to the load provided by the passive excitable nodes. Some of these directions will be explored in future work.

## Acknowledgments

We thank the anonymous referee for critically reviewing our manuscript and providing valuable comments that improved this work. KM is supported by the University Grants Commission, India under the D.S. Kothari Postdoctoral Fellowship Scheme ( BSR/PH/13-14/0044). AB was supported, in part, by the National Science Foundation, USA under DMS-112291. RR acknowledges the support of the Department of Science and Technology, India under DST-SR/S2/JCB/2008.

## References


[1] W. Willinger, R. Govindan, S. Jamin, V. Paxson, S. Shenker, Scaling phenomena in the Internet: critically examining criticality, Proc. Natl. Acad. Sci. USA 99 (2002) 2573.
[2] J. Balthrop, S. Forrest, M.E.J. Newman, M.M. Williamson, Technological networks and the spread of computer viruses, Science 304 (2004) 527.
[3] M.E.J. Newman, Spread of epidemic disease on networks, Phys. Rev. E 66 (2002) 016128.
[4] H. Jeong, B. Tombor, R. Albert, Z.N. Oltvai, A.L. Barabási, The large-scale organization of metabolic networks, Nature 407 (2000) 651.
[5] S. Jain, S. Krishna, A model for the emergence of cooperation, interdependence and structure in evolving networks, Proc. Natl. Acad. Sci. USA 98 (2001) 543.
[6] C. Borgers, N. Kopell, Synchronization in networks of excitatory and inhibitory neurons with sparse random connectivity, Neural Comput. 15 (2003) 509.
[7] D. Terman, D. Wang, Global competition and local cooperation in a network of neural oscillators, Physica D 81 (1995) 148.
[8] S. Kauffman, Metabolic stability and epigenesis in randomly constructed genetic nets, J. Theoret. Biol. 22 (1969) 437.
[9] D. Yang, Y. Li, A. Kuznetsov, Characterization and merger of oscillatory mechanisms in an artificial genetic regulatory network, Chaos 19 (2009) 033115.
[10] R. Guimerà, L. Danon, A.D. Díaz-Guilera, F. Giralt, A. Arenas, Self-similar community structure in a network of human interactions, Phys. Rev. E 68 (2003) 065103(R).
[11] T.W. Pike, M. Samanta, J. Lindström, N.J. Royle, Behavioural phenotype affects social interactions in an animal network, Proc. R. Soc. B 275 (2008) 2515.
[12] R. Albert, I. Albert, G.L. Nakarado, Structural vulnerability of the North American power grid, Phys. Rev. E 69 (2004) 025103(R).
[13] P. Sen, S. Dasgupta, A. Chatterjee, P.A. Sreeram, G. Mukherjee, S.S. Manna, Small-world properties of the Indian railway network, Phys. Rev. E 67 (2003) 036106.
[14] P. Erdös, A. Rényi, On the evolution of random graphs, Publ. Math. Inst. Hung. Acad. Sci. 5 (1960) 17.
[15] A.L. Barabási, R. Albert, Emergence of scaling in random networks, Science 286 (1999) 509.
[16] D. Watts, S. Strogatz, Collective dynamics of 'small-world' networks, Nature 393 (1998) 440.
[17] T.U. Singh, K. Manchanda, R. Ramaswamy, A. Bose, Excitable nodes on random graphs: relating dynamics to network structure, SIAM J. Appl. Dyn. Syst. 10 (2011) 987.
[18] K. Manchanda, T.U. Singh, R. Ramaswamy, Dynamics of excitable nodes on random graphs, Pramana J. Phys. 77 (2011) 803.
[19] Y. Tsubo, J.N. Teramae, T. Fukai, Synchronization of excitatory neurons with strongly heterogeneous phase responses, Phys. Rev. Lett. 99 (2007) 228101.
[20] A. Pomerance, E. Ott, M. Girvan, W. Losert, The effect of network topology on the stability of discrete state models of genetic control, Proc. Natl. Acad. Sci. USA 106 (2009) 8209.
[21] S. Squires, A. Pomerance, M. Girvan, E. Ott, Stability of Boolean networks: The joint effects of topology and update rules, Phys. Rev. E 90 (2014) 022814.
[22] B. Derrida, Y. Pomeau, Random networks of automata: A simple annealed approximation, Europhys. Lett. 1 (1986) 45.
[23] B. Derrida, G. Weisbuch, Evolution of overlaps between Boolean networks, J. Phys. (France) 47 (1986) 1297.
[24] C. Haldeman, J.M. Beggs, Critical branching captures activity in living neural networks and maximizes the number of metastable states, Phys. Rev. Lett. 94 (2005) 058101.
[25] J. Gansert, J. Golowasch, F. Nadim, Sustained rhythmic activity in gap-junctionally coupled networks of model neurons depends on the diameter of coupled dendrites, J. Neurophysiol. 98 (2007) 3450.
[26] K. Manchanda, A.C. Yadav, R. Ramaswamy, Scaling behavior in probabilistic neuronal cellular automata, Phys. Rev. E 87 (2013) 012704.
[27] O. Kinouchi, M. Copelli, Optimal dynamical range of excitable networks at criticality, Nat. Phys. 2 (2006) 348.
[28] M. Müller-Linow, C. Marr, M.-T. Hütt, Topology regulates the distribution pattern of excitations in excitable dynamics on graphs, Phys. Rev. E 74 (2006) 016112.
[29] W. Just, S. Ahn, D. Terman, Minimal attractors in digraph system models of neuronal networks, Physica D 237 (2008) 3186.
[30] J. Greenberg, S. Hastings, Spatial patterns for discrete models of diffusion in excitable media, SIAM J. Appl. Math. 34 (1978) 515.
[31] C. Moore, Majority-vote cellular automata, Ising dynamics, and P-completeness, J. Stat. Phys. 88 (1997) 795.
[32] N. Caporale, Y. Dan, Spike timing-dependent plasticity: a Hebbian learning rule, Annu. Rev. Neurosci. 31 (2008) 25.
[33] B.L. Moss, A.D. Fuller, C.L. Sahley, B.D. Burrell, Serotonin modulates axo-axonal coupling between neurons critical for learning in the leech, J. Neurophysiol. 94 (2005) 2575.
[34] N. Bertschinger, T. Natschläger, Real-time computation at the edge of chaos in recurrent neural networks, Neural Comput. 16 (2004) 1413.
[35] S. Maerivoet, B. De Moor, Cellular automata models of road traffic, Phys. Rep. 419 (2005) 1.
[36] C. Burstedde, K. Klauck, A. Schadschneider, J. Zittartz, Simulation of pedestrian dynamics using a two-dimensional cellular automaton, Physica A 295 (2001) 507.
[37] S. Chatterjee, R. Durrett, Persistence of activity in threshold contact processes, an annealed approximation of random boolean networks, Rand. Struct. Algor. 39 (2011) 228.
[38] D. Larremore, W.L. Shew, J.G. Restrepo, Predicting criticality and dynamic range in complex networks: Effects of topology, Phys. Rev. Lett. 106 (2011) 058101.
[39] F. Nadim, Y. Manor, M.P. Nusbaum, E. Marder, Regulation of a slow STG rhythm, J. Neurosci. 18 (1998) 5053.
[40] G. Buzsáki, A. Draguhn, Neuronal oscillations in cortical networks, Science 304 (2004) 1926.
[41] D.B. Larremore, W.L. Shew, E. Ott, F. Sorrentino, J.G. Restrepo, Inhibition causes ceaseless dynamics in networks of excitable nodes, Phys. Rev. Lett. 112 (2014) 138103.
[42] A. Litwin-Kumar, B. Doiron, Slow dynamics and high variability in balanced cortical networks with clustered connections, Nat. Neurosci. 15 (2012) 1498.